HiSST: International Conference on
High-Speed Vehicle Science Technology
26–29 November 2018, Moscow, Russia

Application of RANS/LES Hybrid Method in Simulation of Supersonic Base Base Flow

FU Weijia[1], MA Jingzhong[2], LI Jie[3], ZHANG Lu[4]

Abstract

Two methods DDES, ZDES based on $k-\omega$ SST shear stress transport model with compressibility correction are applied in numerical simulation of supersonic base flow, respectively. Third-order MUSCL-Roe and fifth-order WENO-Roe spatial scheme are used to investigate the numerical dissipation effects. The calculated results are compared with experimental data. It shows that fifth-order WENO-Roe scheme is more validated than third-order MUSCL-Roe scheme. The comparison of results obtained by DDES and ZDES are also conducted. The results show that ZDES method is better than DDES method in regions near the wall. The complex flow mechanism of supersonic base flow is comprehensively understood, which provides references for the application of RANS/LES hybrid method in the simulation of unsteady supersonic flow.

Keywords: *supersonic base flow; DDES method; ZDES method; numerical simulation*

Nomenclature

a_∞ – free stream sound speed
c_p – local pressure coefficient
D – cylinder base diameter
Δt – integration time
M_∞ – free stream Mach number
p_∞ – free stream static pressure
R – cylinder base radius
Re – Reynolds number
r – radial coordinate
t – Temperature
U_∞– free stream velocity
U – time averaged velocity
Y – distance from the wall
Superscripts
$+$ – wall unit quantity

1. Introduce

Slender aircraft such as projectile or missile is experience massive separation at the base leading to a dramatic increase in drag when supersonic flight. Modern supersonic aircraft design requires high stability and control performance. The achievement of the advance in supersonic aircraft requires advanced design concept which is based on a comprehensive and accurate estimation of supersonic base flowfield.

For many years, various experimental investigations of a supersonic base flow have been performed. Herrin and Dutton[1] studied the complex flow structure near wake of the supersonic base flow at M=2.5 through wind tunnel experiment. Bourdon[2] investigated the supersonic base flow with scattering imaging technique, and obtained planar flow visualization image of the instantaneous flow near the wake region. However, for the experimental approach, the support sting equipment in the wind tunnel will affect the flowfield, it destroys the flow structure behind the test model. Although the

[1] *AVIC Jiangxi Hongdu Aviation Industry Group, Nanchang, China, E-mail mm007@163.com*
[2] *AVIC Jiangxi Hongdu Aviation Industry Group, Nanchang, China*
[3] *School of Aeronautics, Northwestern Polytechnical University, Xi'an, China, E-mail lijieruihao@163.com*
[4] *School of Aeronautics, Northwestern Polytechnical University, Xi'an, China, E-mail zhanglu405@126.com*

experimental data can be compensate by empirical methods, there is still a lack of validation research on the reliability of these empirical methods.

As a result, researchers began to use Computational Fluid Dynamics (CFD) method to study the supersonic base flows[3, 4]. However, it is difficult to predict the supersonic base flow by solving the Reynolds-average Navier-Stokes (RANS) equation due to the limited simulation capability of RANS method. As the development of computer technology and the detached eddy simulation (DES) method, the simulation of supersonic base flow is now feasible. The DES method combines the advantages of RANS method and large eddy simulation (LES) method. The DES method uses a RANS turbulence model to resolve the smallest scales in the boundary layer region, while the largest scales outside the boundary layer are resolved by LES.

Researchers have adopted various RANS/LES methods to predict the supersonic base flows[5-9]. Forsythe et al. [6] applied the DES method based on SA and SST turbulence model, and introduced compressible corrections, to predict the flowfild of the supersonic base. Temporal-averaged mean flowfields are presented and a relatively good agreement with experimental data is observed when a fine grid of approximately 2.8×10^6 points is used. Baurle et al. [7] applied a subregional RANS/LES hybrid method, which combines SST model with one-equation SGS model, to predict supersonic base flow. Kawai and Fujii [8] adopted the RANS/LES method which combines BL and Smarisky model. The method has better performance in calculation accuracy and efficiency by comparison with LES, MILES and RANS results and the experiments in detail.

In present work, Delayed Detached Eddy Simulation (DDES) [10,11] and Zomal Detached Eddy Simulation (ZDES)[20,21] based on the k-ω shear stress transport (SST) turbulence model are applied to predicted the supersonic base flowfiled. The compressible corrections [12] are introduced. The influence of numerical dissipation effect on the supersonic base flow and sensitivities of mesh resolution are investigated. The results simulated by both DDES and ZDES methods are also compared.

2. Numerical Approach

In present study, the central finite volume method is applied, a second-order fully implicit LU-SGS-τTS algorithm is applied for time discretization, and the Roe scheme based on the third-order MUSCL (Monotone Upstream-centred Schemes for Conservation Law) and the fifth-order WENO (Weighted Essentially Non-oscillatory) interpolation are used for spatial discretization. The entropy corrections proposed by Harten are also introduced in current study.

For the numerical simulation of supersonic base flow, Forsythe et al. [6] compared the results of one-equation SA model and two-equation SST model, and the results obtained by SST model is obviously far better than that of SA model. In this paper, SST model is used as the basic turbulence model of RANS/LES hybrid method. More details of the RANS/LES methods applied in this paper are in Refs [13-21].

The numerical simulation is based on Herrin and Dutton's experiments[1]. The Mach number of free flow at the inlet is $M_\infty = 2.46$, the inlet pressure is $p_\infty = 31415P_a$, the temperature is $T = 145k$, the diameter of the experimental cylinder is $D = 63.5mm$, and the Reynolds number based on the diameter of the cylinder is $Re = 2.858 \times 10^6$.

The velocity distribution at the inlet is matched with the experimental data. The cylinder surface is treated as no slip, the outlet is treated as an interpolation boundary, and the far field is a non-reflective boundary. Based on the cylinder diameter D and sound speed a_∞, the dimensionless time step is $\Delta t = 0.001$. Twenty sub-iterations are taken in each time step. Time-averaged results are obtained by averaging flowfileds about 30000 steps of unsteady flow simulations.

3. Results and discussion

A multi-block structured grid is used. The whole computational domain size is $5D \times 9D$(cylinder base diameter $\times$ height), it extends $4D$ upstream $5D$ downstream from the base plane. The mesh near the bottom of the cylinder and in the downstream region is refined. The average first spacing $y^+$is less than 1. The computational grids are shown in Figures 1 and 2.

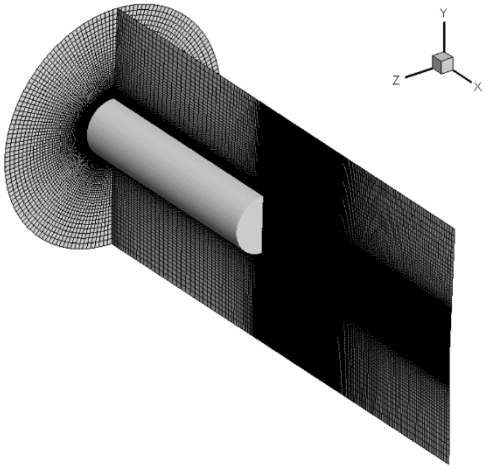

Fig 1. Computational grid in 3D view

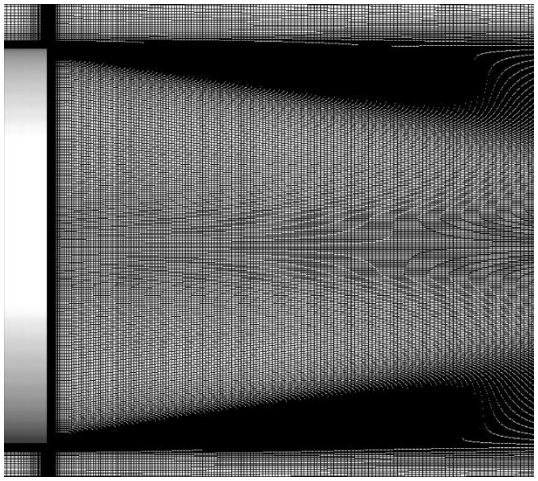

Fig. 2 Computational grid in detail view

3.1. Effect of grid density

In order to evaluate the simulation sensitivity to the spatial resolution to clarify an adequate mesh solution for the hybrid method, three sets of computational grids are generated, all of which adopt the same topological type and the same first-layer mesh size. The grid densities of the coarse, fine and extremely fine grids are 8×10^6 (Mesh-C), 2×10^7 (Mesh-F) and 3×10^7 (Mesh-EF), respectively. The DDES method is adopted to solve the three sets of grids respectively with the third-order MUSCL-Roe scheme.

The time-averaged centerline velocity distributions predicted by different density grids are compared (as shown in Fig. 3.). The peak reverse velocity predicted by the three sets of grid calculation is higher than the experimental data. The peak reverse velocity predicted by coarse gird is obviously over-predicted, and the reattachment point is under predicted by 16.10%, located at nearly *X/R=2.24* compared to the experiment value of 2.67. The peak reverse velocitys predicted by fine gird and extremely fine gird are better, and the reattachment point is under predicted by 9.73%, located at nearly *X/R=2.41* compared to the experiment value of 2.67.

From the results of the grid sensitivity study, spatial resolution of the fine grid is considered to have an adequate mesh resolution to simulate essential features of the base flow that we focus on with the RANS/LES hybrid methodology. Therefore, the fine grid is used in the present study.

3.2. Effect of numerical scheme

Accurate schemes are preferred to lower the numerical dissipation when RANS/LES hybrid methods are used. Two DDES methods based on the SST turbulence model simulations are performed to evidence its influence on the prediction. One is performed using the third-order MUSCL-Roe scheme while the other is using fifth-order WENO-Roe scheme.

Time-averaged results of third-order MUSCL scheme and fifth-order WENO scheme computations are discussed. The boundary layer profiles are plotted in Fig. 4. Both the predicted profiles match the experimental data well. The present DDES method predicts the boundary layer profile reasonably well under the current mesh resolution.

Time-averaged base pressure distributions along the base surface are compared with the experiment in Fig.5. Both the base pressure coefficients obtained by third-order MUSCL scheme and fifth-order WENO scheme are clearly overpredicted. When the prediction accuracy of the base pressure distributions are compared between the results with the third-order MUSCL scheme and the results with the fifth-order WENO scheme, better prediction is obtained by using the fifth-order WENO scheme computation. The mean averaged base pressure coefficient is approximately -0.091 compare to the experimental value of -0.102. As the decrease of the numerical dissipation, the prediction accuracy of the base pressure is improved remarkably.

The centerline velocity plotted in Fig.6. exhibits a similar behavior as the numerical dissipation decreased. The third-order MUSCL scheme is again underresolved, giving a high peak reverse velocity

too close to the base. The fifth-order WENO scheme gives a much better result for centerline velocity. The peak reverse velocity and reattachment point are predicted well compared to the experiment.

Time-averaged axial and radial velocity distributions at the location of *x/R=0.6299*, *x/R=1.2598* and *x/R=1.8898* planes behind the base separation are compared with experiment in detail in Figs 7 and 8. In the third-order MUSCL scheme computation, due to the high numerical dissipation, width of the free shear layer is predicted thinner than the fifth-order WENO scheme and experiment. The predicted position of the shear layer exists rather inside compared to the fifth-order WENO scheme and experiment. Better results are obtained by using the fifth-order WENO scheme computation. These results indicate that accurate prediction of the supersonic base flows requires adequate spatial discretization scheme to accurately resolve the approaching boundary layer developing on the cylinder lateral surface even if the separation is fixed at the base edge.

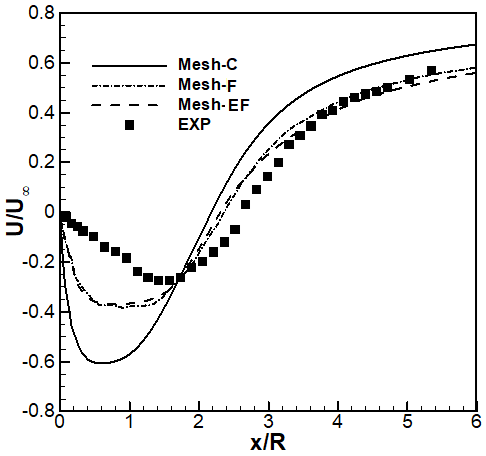

Fig. 3 Time-averaged centerline velocity

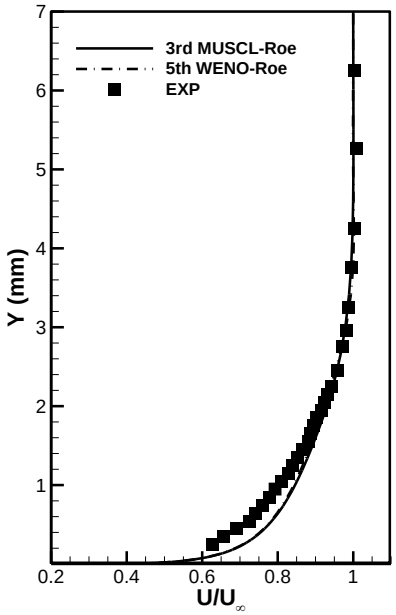

Fig. 4 Boundary layer profile 1mm prior the base

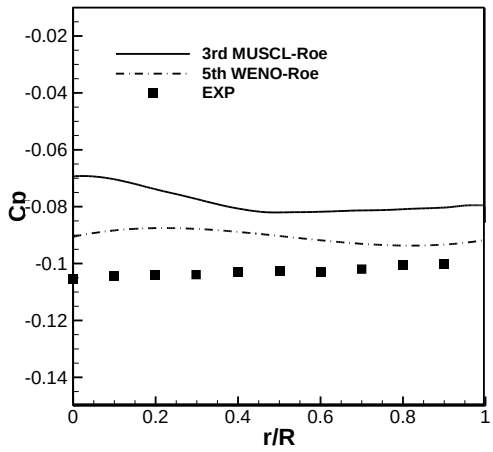

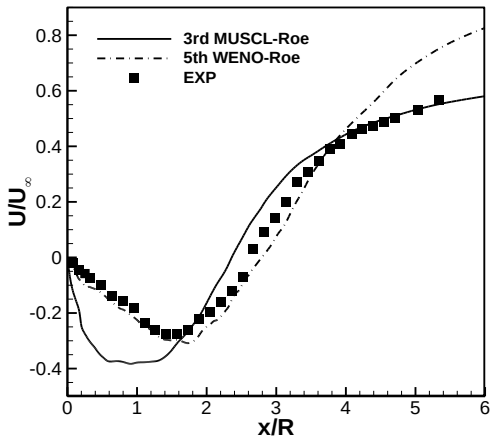

Fig. 5 Time-averaged base pressure coefficient **Fig. 6** Time-averaged centerline velocity

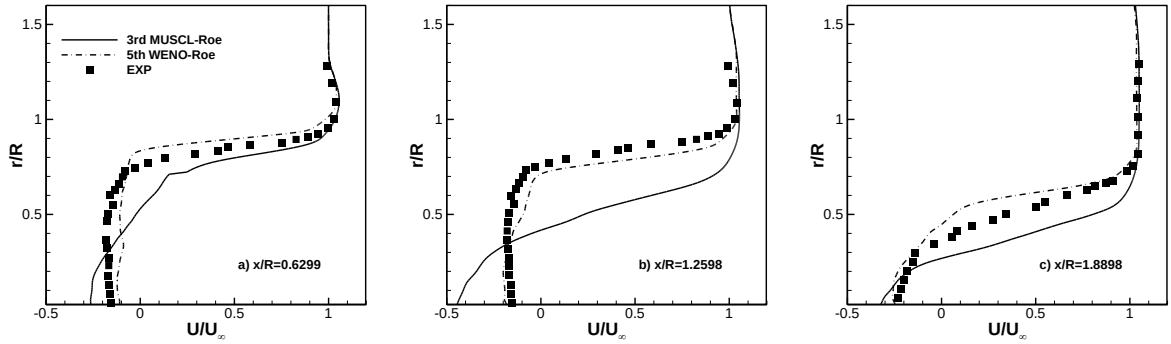

Fig. 7 Time-averaged axial velocity profile

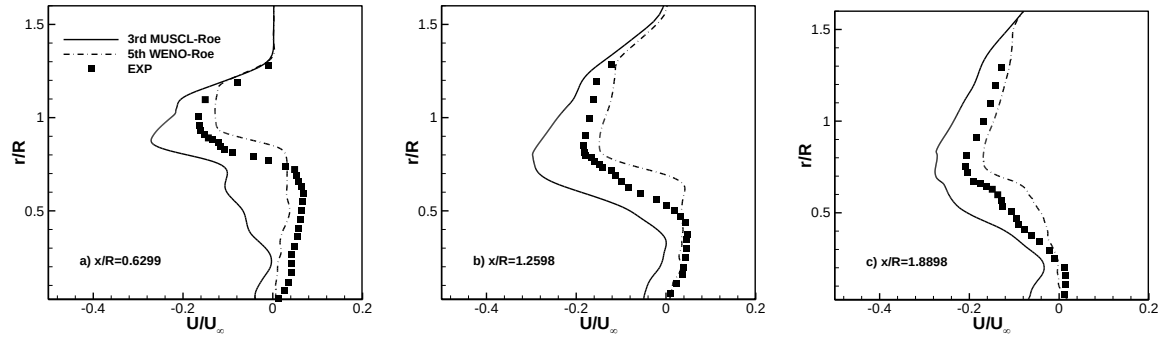

Fig. 8 Time-averaged radial velocity profile

Fig. 9 shows the instantaneous plot of vorticity contours in a cross-plane behind the base for the two spatial schemes. In both of the computations, the turbulent structures are well resolved. Compared with third-order MUSCL scheme, more small-scale turbulence structures can be captured by using the fifth-order WENO scheme.

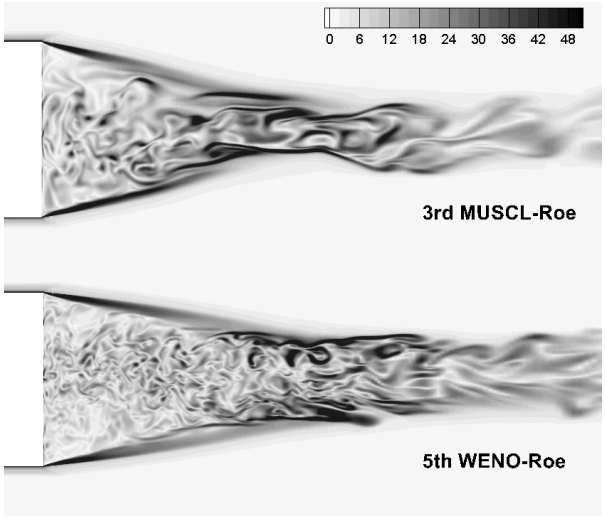

Fig. 9 Instantaneous vortices

3.3. DDES and ZDES results

To investigate the capabilities of advanced unsteady methods to predict the supersonic base flows. Two RANS/LES methods based on the SST turbulence model simulations are performed One is performed using DDES method while the other is using ZDES method.

A comparison of measured and computed boundary layer velocity profiles on the cylinder lateral surface 1 mm prior the base is shown in Fig. 10. The results obtained by DDES and ZDES methods look quite similar. The boundary layer velocity profiles as well as the thickness of the boundary layer predicted by DDES and ZDES methods are in good agreement with the experimental data.

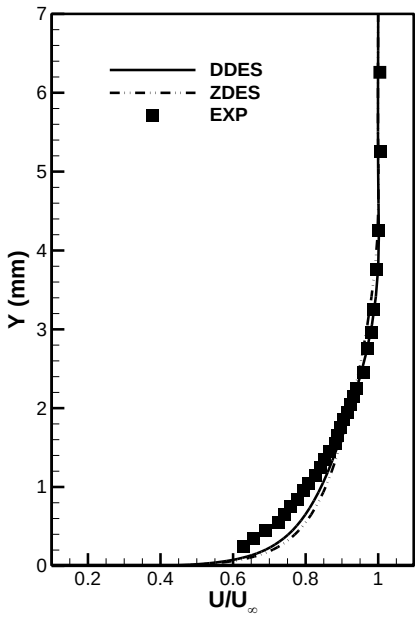

Fig. 10 Boundary layer profile 1mm prior the base

Time-averaged base pressure distributions along the base surface are compared with the experiment in Fig.11. DDES and ZDES display a flat pressure profile which agrees well with the experimental data. The DDES method under predicts the base pressure by 10.78% compare to the experimental value of -0.102. The ZDES results show excellent agreement with the experimental data. It can be concluded that prediction accuracy of the base pressure using the ZDES method is reasonably well and improved remarkably compared with the results of the DDES.

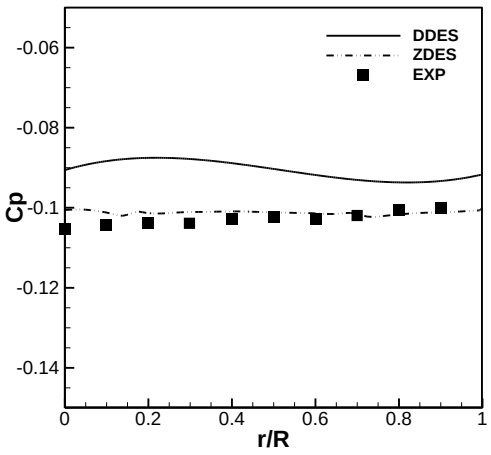

Fig. 11 Time-averaged base pressure coefficient

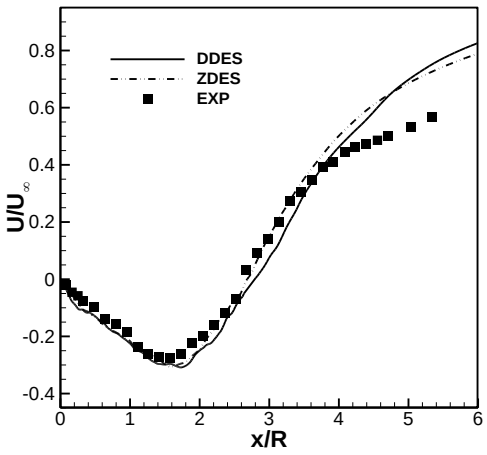

Fig. 12 Time-averaged centerline velocity

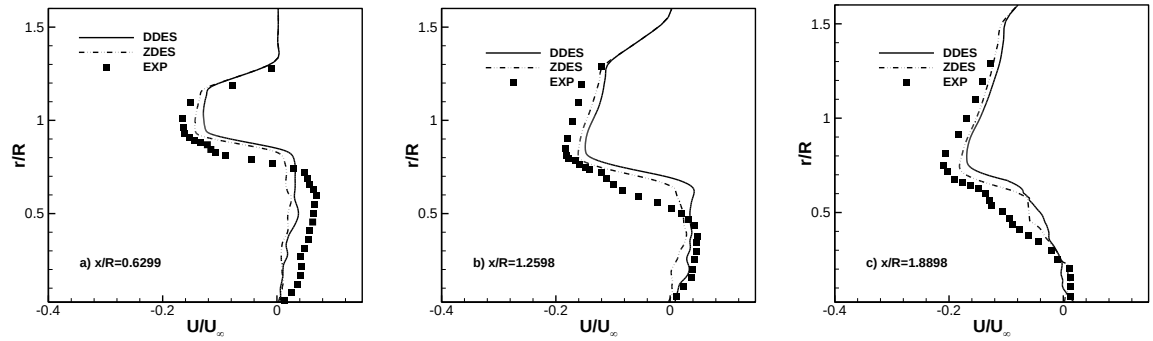

Fig. 13 Time-averaged axial velocity profile

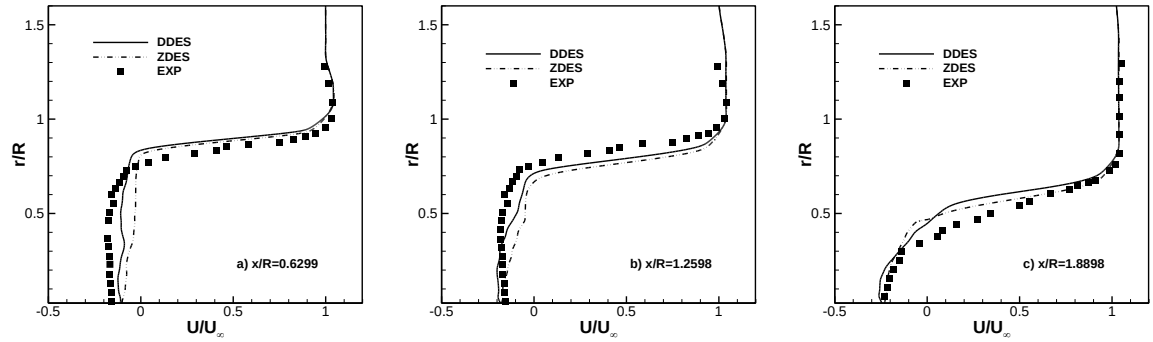

Fig. 14 Time-averaged Radial velocity profile

Fig.12. shows a comparison of time-averaged centerline velocity. The peak reverse velocity and reattachment point obtained by DDES and ZDES methods are in good agreement with the experimental data. However, after the attachment point, the axial velocity distributions obtained by DDES and ZDES methods are far from the experimental data. The fact that both results start to deviate from the experimental data around x/R=4.0 may be due to the gradual increase of the grid size in the downstream wake region as the distance from the base increases.

Axial and radial time-averaged velocity distributions at the location of x/R=0.6299, x/R=1.2598 and x/R=1.8898 planes behind the base separation are compared with experiment in detail in Figs 13 and 14. At the location of x/R=0.6299 and x/R=1.2598, the shear layers predicted by the two methods are all in the region of r/R=0.8~1.0, which are in good agreement with the experimental results. In the recirculation region (r/R < 0.8), the results of DDES and ZDES are also close to the experimental values. Further downstream, at the location of x/R=1.8898, near the reattachment region, the shear layer heights obtained by DDES and ZDES methods are near r/R=0.5, which is in good agreement with the experimental data.

Fig. 15 compares the instantaneous plot of vorticity contours in a cross-plane behind the base predicted by DDES and ZDES methods. Unsteady shear-layer roll-up, large eddy motions to the downstream and small eddy motions inside the recirculation region behind the base separation are observed, and the ZDES can capture more details of the flow field compare with the DDES results.

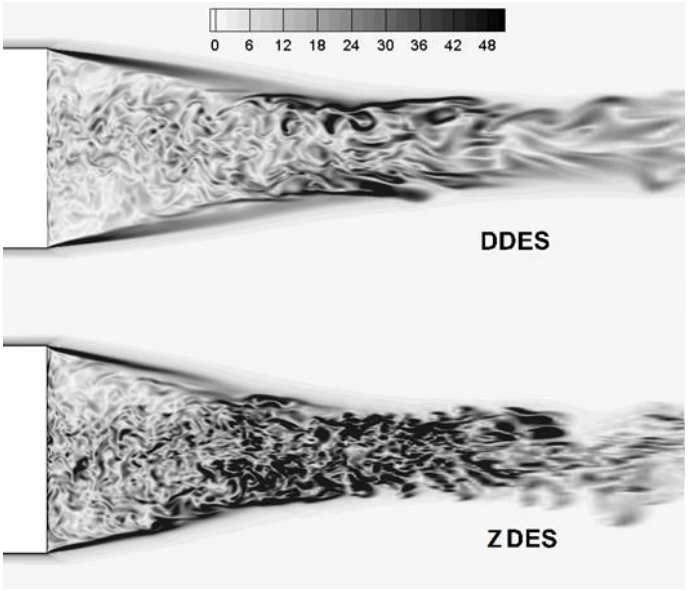

Fig. 15 Instantaneous vortices

4. Conclusions

The DDES and ZDES methods based on the k-ω SST turbulence model combined with compressibility correction are used to simulate the supersonic base flow. To accurately simulate the supersonic base flow, three sets of grids are used to explore the effect of grid density by using DDES method combined with third-order MUSCL-Roe scheme.

The third-order MUSCL-Roe and fifth-order WENO-Roe spatial discrete schemes are used to study the effect of numerical dissipation on flow field calculation. Both the third-order MUSCL-Roe and fifth-order WENO-Roe scheme can predict the boundary layer before separation. As the decrease of the numerical dissipation, the prediction accuracy of the base pressure is improved remarkably by using the fifth-order WENO-Roe scheme. The results such as peak reverse velocity, reattachment point, and the width and position of the free shear layer obtained by fifth-order WENO-Roe scheme are better third-order MUSCL-Roe scheme. The results simulated by both DDES and ZDES methods are also compared.

The boundary layer velocity profiles, axial and radial time-averaged velocity predicted by DDES and ZDES methods are in good agreement with the experimental data. Prediction accuracy of the base pressure using the ZDES method is reasonably well and improved remarkably compared with the results of the DDES. The ZDES can capture more details of the flow field compare with the DDES results.

References

1. HERRIN J L, DUTTON J C. Supersonic base flow experiments in the near wake of a cylindrical afterbody[J]. AIAA Journal, 1994, 32(1): 77–83.
2. BOURDON C J, DUTTON J C. Planar visualizations of large-scale turbulent structures in axisymmetric supersonic separated flows[J]. Physics of Fluids, 1999, 11(1): 201–213.
3. Benay R. and Servel P. Two-Equation k– σ Turbulence Model: Application to a Supersonic Base Flow[J]. AIAAJournal, Vol.39, No.3, March 2001, pp.407-416.
4. Papp J. L. and Ghia K. N. Application of the RNG Turbulence Model to the Simulation of Axisymmetric Supersonic separated Base Flows[J]. AIAA Paper 2001-0727, Jan. 2001.
5. Fureby C., Nilsson Y. and Andersson K. Large Eddy Simulation of Supersonic Base Flow[J]. AIAA Paper 99-0426, Jan. 1999.

6. FORSYTHE J R, HOFFMANN K A, CUMMINGS R M, et al. Detached-eddy simulation with compressibility corrections applied to a supersonic axisymmetric base flow[J], Journal of Fluids Engineering, 2002, 124: 911–923.
7. Baurle A. R. and Tam -J. C. Hybrid Simulation Approach for Cavity Flows: Blending, Algorithm, and Boundary Treatment Issues[J]. AIAAJournal, Vol.41, No.8, August 2003, pp.1463-1480.
8. KAWAI S, FUJII K, Computational study of supersonic base flow using hybrid turbulence methodology[J]. AIAA Journal, 2005, 43(6): 1256-1275.
9. SIMON F, DECK S, GUILLEN P, et al. Reynolds-averaged navier-stokes/large-eddy simulations of supersonic base flow[J]. AIAA Journal, 1994, 44(11): 2578–2590.
10. SPALART P R, DECK S, SHUR M, et al. A new version of detached-eddy simulation, resistant to ambiguous grid densities[J]. Theoretical. and Computational Fluid Dynamics, 2006, 20(3): 181–195.
11. SHUR M L, SPALART P R, STRELETS M, et al. A hybrid RANS-LES approach with delayed-DES and wall-modeled LES capabilities[J]. International Journal of Heat and Fluid Flow, 2008, 29(6): 1638-1649.
12. HARTEN A, HYMAN J M. Self-adjusting grid methods for one-dimensional hyperbolic conservation laws[J]. Journal of Comput.Physics, 1983, 50(2): 235-369.
13. ZHANG Lu, LI Jie. Numerical simulations of supersonic base flow field based on RANS/LES approaches[J]. Acta Aeronatica et Astronautica Sinica, 2013, 34(7): 1531-1537.
14. MENTER F R. Two-equation eddy viscosity turbulence models for engineering applications[J]. AIAA Journal, 1994, 32(8): 1598-1605.
15. SUZEN Y B, HOFFMANN K A. Investigation of supersonic jet exhaust flow by one- and two-equation turbulence models. AIAA 98-0322[R], Reston: AIAA, 1998.
16. GRITSKEVICH M S, GARBARUK A V, SCHUTZE J, et al. Development of DDES and IDDES formulations for the k-ω shear stress transport model. Flow[J], Turbulence and Combustion, 2012, 88(3): 431-449.
17. Van Leer B, Towards the Ultimate Conservative Difference Scheme V: A Second Order Sequel to Godunov's method[J], Journal of Computational Physics, 1979, 32: 101-136.
18. BORGES R, CARMONA M, COSTA B, et al. An improved weighted essentially non-oscillatory scheme for hyperbolic conservation laws[J]. Journal of Computational Physics, 2008, 227(6):3191-3211.
19. JIANG G S, SHU C W, Efficient implementation of weighted ENO schemes[J], Journal of Computational Physics, 1996, 126(1): 202-228.
20. Deck, S., "Zonal-Detached Eddy Simulation of the Flow around a High Lift Configuration," AIAA Journal, Vol. 43, No. 11, 2005, pp. 2372–2384.
21. Menter, F.R., Kuntz, M.: A zonal SST-DES formulation. DES workshop, St. Petersburg, Russia (2003)